

Multi-Objective Optimization of CMT-WAAM Inconel 718 Thin Walls Using TOPSIS and GRA: A Comparative Study of Entropy and Equal Weighting Schemes

Phung Chi Tinh¹, Le Van Thao², Do Manh Tung¹, Mai Dinh Si², Nguyen Van Son², Tran Van Chau², Bui Manh Cuong¹, Doan Tat Khoa¹, Le Xuan Hung¹

¹Faculty of Mechanical Engineering, Le Quy Don Technical University, Hanoi, Vietnam

²Advanced Technology Center, Le Quy Don Technical University, Hanoi, Vietnam

*Corresponding author: phungchitinh.pct@gmail.com.

Abstract— The fabrication of Inconel 718 thin-walled components using Cold Metal Transfer-based Wire Arc Additive Manufacturing (CMT-WAAM) requires a careful balance between deposition productivity and surface quality. This study presents a comparative multi-objective optimization of process parameters—wire feed speed (wfs) and travel speed (v)—for 20-layer thin walls, focusing on three key responses: Effective Width (EW), Total Height (TH), and Surface Roughness (Sa). Two prominent multi-criteria decision-making methods, TOPSIS and Grey Relational Analysis (GRA), were implemented under two distinct weighting scenarios: (1) objective weights derived from the Entropy Weight Method (EWM), and (2) equal weights (1/3 for each response).

Experimental results from a full factorial design of nine runs were analyzed. Statistical analysis via ANOVA revealed that wfs is the dominant factor affecting EW (65.45% contribution), while v primarily governs TH (59.72%) and Sa (69.67%). Under entropy weights (EW: 0.797, TH: 0.135, Sa: 0.068), both TOPSIS and GRA consistently identified Run 7 (wfs = 6 m/min, v = 40 cm/min) as the optimal condition, achieving the highest performance index (0.9780) and grey relational grade (0.9547). Under equal weights, Run 7 remained optimal in both methods, confirming its robustness. The only discrepancy was observed in GRA's suboptimal ranking, where Run 6 ranked second due to its superior surface roughness, indicating higher sensitivity of GRA to the surface quality criterion.

The perfect convergence between TOPSIS and GRA under both weighting schemes confirms the robustness of the proposed optimization framework. This research provides a scientific basis for selecting appropriate weighting strategies in multi-objective optimization of CMT-WAAM processes for nickel-based superalloys.

Keywords— CMT-WAAM, Inconel 718, TOPSIS, Grey Relational Analysis (GRA), Entropy Weight Method, Multi-objective Optimization.

I. INTRODUCTION

Wire Arc Additive Manufacturing (WAAM) has emerged as a transformative technology for fabricating large-scale metallic components due to its high deposition efficiency, low equipment cost, and material utilization rates exceeding 90% [1,2]. Among various arc-based directed energy deposition processes, Cold Metal Transfer (CMT) has gained particular attention for manufacturing nickel-based superalloys because of its low heat input, spatter-free droplet transfer, and enhanced process stability [3,4]. Inconel 718, a precipitation-hardened

superalloy widely employed in aerospace and energy sectors, exhibits excellent high-temperature strength and corrosion resistance. However, its poor machinability, high work-hardening rate, and susceptibility to thermal cracking pose significant challenges during conventional processing [5,6].

In CMT-WAAM of Inconel 718 thin-walled structures, the geometric characteristics—particularly effective width (EW) and total height (TH)—directly determine the dimensional accuracy and structural integrity of the final component [7,8]. Surface roughness (Sa) is equally critical as it influences post-processing requirements and fatigue performance [9,10]. The interaction between wire feed speed (wfs) and travel speed (v) fundamentally governs the heat input, material deposition rate, and molten pool dynamics, thereby affecting all three responses simultaneously [11,12]. Previous studies have demonstrated that wfs primarily controls lateral spreading and bead width, while v dominates vertical buildup and surface morphology [13,14]. However, optimizing these parameters to simultaneously maximize EW and TH while minimizing Sa represents a classic multi-objective optimization problem with inherent trade-offs [15].

Multi-criteria decision-making (MCDM) methods have been increasingly applied to resolve such conflicting objectives in additive manufacturing. Among these, the Technique for Order of Preference by Similarity to Ideal Solution (TOPSIS) and Grey Relational Analysis (GRA) are two widely adopted approaches [7,10]. TOPSIS ranks alternatives based on their geometric distances to the positive and negative ideal solutions, while GRA evaluates the degree of grey relational grade between each alternative and a reference sequence [16]. A critical yet often overlooked aspect in both methods is the assignment of criterion weights. The Entropy Weight Method (EWM) provides objective weights based on the inherent dispersion of experimental data, whereas equal weighting (1/3 for each response) offers a subjective alternative that treats all criteria with identical importance [16].

Despite the individual applications of TOPSIS and GRA in manufacturing optimization [7,10,13], a systematic comparison of these two methods under different weighting schemes—objective (entropy-based) versus equal—has not been reported for CMT-WAAM of Inconel 718 thin walls. Therefore, this

study aims to: (1) apply TOPSIS and GRA to optimize wfs and v for maximizing EW and TH while minimizing Sa; (2) compare the ranking results obtained with entropy weights versus equal weights (1/3 each); and (3) discuss the implications of weighting selection on the final optimal parameter set. The experimental data from a full factorial design (9 runs) of 20-layer Inconel 718 walls fabricated by CMT-WAAM serves as the basis for this comparative investigation.

II. EXPERIMENT

1. Materials and CMT-WAAM System

The workpiece material used in this study was Inconel 718 solid wire with a diameter of 1.2 mm (KW-M718, Kiswel Ltd.). The chemical composition of the filler wire is presented in Table I. A low-carbon structural steel plate (EN 10025-2, S235JR) with dimensions of 200×100×6 mm was employed as the substrate. Prior to deposition, the substrate surfaces were sandblasted and cleaned with acetone to remove oxides, oil, and contaminants, ensuring stable arc ignition and proper metallurgical bonding.

TABLE I. Chemical composition of Inconel 718 wire and S235JR steel (wt.%)

Materials	C	Mn	Si	Cr	Mo	Nb+Ta
Inconel 718	≤ 0.08	≤ 0.35	≤ 0.35	17.0 – 21.0	2.8 – 3.3	4.75 – 5.50
S235JR	≤ 0.17	≤ 1.4	≤ 0.5	≤ 0.3	≤ 0.08	≤ 0.05
Materials	Ti	Al	Co	Ni	Fe	
Inconel 718	0.65 – 1.15	0.20 – 0.80	≤ 1.0	50.0 – 55.0	Bal.	
S235JR	≤ 0.03	≤ 0.02	-	≤ 0.3	Bal.	

The CMT-WAAM system integrated a six-axis industrial robot (FANUC Arc Mate 100iD) with a CMT power source (Fronius TPS 400i). The process operated in standard Cold Metal Transfer (CMT) mode with a contact-tip-to-work distance of 15 mm and a torch angle of 90° relative to the substrate surface. High-purity argon (99.999%) was used as shielding gas at a constant flow rate of 15 L/min to prevent atmospheric contamination of the molten pool. All depositions were performed under ambient conditions without external preheating.



Figure 1. The CMT-WAAM system, including a 6-axis Fanuc robot arm, robot control cabinet, and a CMT power source (TPS400i)

2. Experimental Design

For CMT power sources, the welding current and voltage are synergically linked to the wire feed speed (wfs). Therefore, wire feed speed (wfs) and travel speed (v) were selected as the

two primary input variables. A full factorial experimental design with three levels for each parameter was employed, resulting in nine experimental runs. The selected parameter ranges (Table II) were determined based on the wire manufacturer's recommendations and preliminary trial tests to ensure stable droplet transfer and defect-free deposition.

TABLE II. Levels of input parameters

Parameters	Levels		
wfs (m/min)	4	5	6
v (cm/min)	40	50	60

For each experimental run, a 20-layer thin-wall structure was fabricated using a unidirectional deposition strategy with alternating travel direction between layers to maintain geometric balance. The deposition length was 100 mm for each layer. A constant interlayer dwell time of 60 seconds was applied to control heat accumulation and allow partial cooling of the previously deposited layer. The number of 20 layers was selected to represent a typical multi-layer WAAM structure where thermal accumulation effects become significant.

3. Geometric and Surface Roughness Measurement

After deposition, the wall geometry was characterized by three responses: effective width (EW), total height (TH), and areal surface roughness (Sa). The total width (TW) and surface profile parameter (Sz) were initially measured to calculate the effective width (EW), which represents the functional deposition width by excluding edge irregularities. The effective width was calculated as:

$$EW = TW - Sz_{(left)} - Sz_{(right)}$$

where $Sz_{(left)}$ and $Sz_{(right)}$ are the maximum heights of surface irregularities on the left and right sides, respectively, obtained from 3D surface topography.

The surface morphology of the walls was captured using an ATOS optical 3D scanning system (GOM GmbH, Germany). Data from a central region of interest (60×20 mm) were processed in OmniSurf 3D software to determine Sa parameters according to ISO 25178. The total wall height (TH) and total width (TW) were measured at 5 mm intervals along the wall length (excluding the arc start and end regions of 20 mm from each end) using digital calipers with an accuracy of ± 0.01 mm. Subsequently, the average values of TH and TW were taken for analysis.

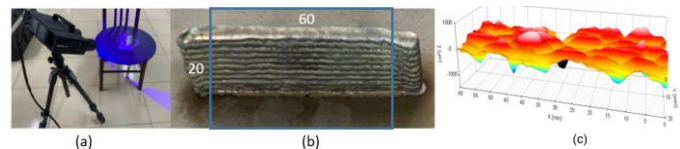


Figure 2. Data acquisition: (a) 3D scanning setup using the ATOS optical system for surface geometry acquisition; (b) Stable region; (c) 3D surface morphology

4. Experimental Data

The complete experimental design matrix and measured responses for the nine runs are summarized in Table III. Each experimental condition was performed once due to material and time constraints, which is consistent with typical WAAM optimization studies. These data serve as the input decision

matrix for the subsequent TOPSIS and GRA optimization procedures.

TABLE III. Experimental design matrix and measured responses

Run No.	wfs (m/min)	v (cm/min)	EW (mm)	TH (mm)	Sa (µm)
1	4	40	5.71	36.26	147.91
2	4	50	5.27	33.93	142.35
3	4	60	4.73	32.11	139.69
4	5	40	6.60	38.59	153.84
5	5	50	6.49	35.64	148.79
6	5	60	5.52	33.86	137.37
7	6	40	8.30	39.91	159.42
8	6	50	7.06	37.58	147.02
9	6	60	6.34	35.56	144.27

As observed from Table III, increasing wire feed speed generally increases both EW and TH due to higher material deposition rates. Conversely, increasing travel speed reduces both EW and TH because of decreased heat input per unit length. Surface roughness exhibits a more complex behavior, with the highest Sa values observed at high wfs and low v (Run 7: 159.42 µm) due to excessive heat accumulation and molten pool instability.

III. METHODOLOGY

A. Definition and Optimization Framework

The multi-response optimization problem in this study aims to determine the optimal combination of wire feed speed (wfs) and travel speed (v) that simultaneously maximizes effective width (EW) and total height (TH) while minimizing surface roughness (Sa). This can be formally expressed as:

Find {wfs and v} to maximize {EW and TH} while minimize Sa

Subject to: $4 \leq wfs \leq 6$ m/min and $40 \leq v \leq 60$ cm/min.

To resolve this conflicting objective problem, two widely adopted multi-criteria decision-making (MCDM) methods—TOPSIS and Grey Relational Analysis (GRA)—were implemented independently. For each method, two distinct weighting schemes were applied: (1) objective weights derived from the Entropy Weight Method (EWM), and (2) equal weights (1/3 for each response).

B. Entropy Weight Method (EWM)

The Entropy Weight Method is an objective weighting technique that determines criterion importance based on the inherent dispersion of experimental data. Criteria with higher variability are assigned larger weights as they convey more information [16]. The EWM procedure consists of four steps:

Step 1: Normalization of the decision matrix. For beneficial criteria (EW, TH), the normalized value r_{ij} is calculated as:

$$r_{ij} = \frac{x_{ij}}{\sum_{i=1}^m x_{ij}}, i = 1, \dots, m; j = 1, \dots, n \quad (1)$$

For cost criteria (Sa), the normalized value is calculated using the same formula, where x_{ij} represents the original value of the i -th experimental run for the j -th response indicator, $m = 9$ is the number of experimental runs, and $n = 3$ is the number of responses.

Step 2: Calculation of the entropy value e_j . The entropy value characterizes the uncertainty of information for each criterion:

$$e_j = -\frac{1}{\ln m} \sum_{i=1}^m r_{ij} \ln r_{ij}, 0 \leq e_j \leq 1 \quad (2)$$

Step 3: Calculation of the diversification degree d_j . This represents the useful information provided by the j -th criterion:

$$d_j = 1 - e_j \quad (3)$$

Step 4: Determination of the final objective weights w_j . The weight for each response is obtained by normalizing the diversification degree:

$$w_j = \frac{d_j}{\sum_{j=1}^n d_j} \quad (4)$$

For the equal weighting scheme, all three responses are assigned identical importance: $w_j = 1/3 \approx 0.3333$ for EW, TH, and Sa.

C. TOPSIS Method

The Technique for Order of Preference by Similarity to Ideal Solution (TOPSIS) is a classical MCDM method that ranks alternatives based on their geometric distances to the positive ideal solution (PIS) and negative ideal solution (NIS) [16]. The alternative closest to the PIS and farthest from the NIS is considered optimal. The TOPSIS procedure is implemented as follows:

Step 1: Construction of the decision matrix (x_{ij}) a matrix is formed with m experimental runs and n response indicators (EW, TH, and Sa).

Step 2: Normalization of the decision matrix (r_{ij}) to transform different units (mm and µm) into dimensionless values, vector normalization is applied:

$$r_{ij} = \frac{x_{ij}}{\sqrt{\sum_{i=1}^m x_{ij}^2}}, i = 1, \dots, m; j = 1, \dots, n \quad (5)$$

Step 3: Calculation of the weighted normalized decision matrix (v_{ij}). The normalized values are multiplied by the objective weights (w_j) derived from the EWM method:

$$v_{ij} = w_j \cdot r_{ij} \quad (6)$$

Step 4: Determination of Positive Ideal Solution (A^+) and Negative Ideal Solution (A^-):

For benefit criteria (EW, TH):

$$v_j^+ = \max(v_{ij}), v_j^- = \min(v_{ij}) \quad (7)$$

For cost criteria (Sa):

$$v_j^+ = \min(v_{ij}), v_j^- = \max(v_{ij}) \quad (8)$$

Step 5: Calculation of Euclidean distances (D_i^+ and D_i^-). The distance of each alternative from the PIS and NIS is calculated as follows:

$$D_i^+ = \sqrt{\sum_{j=1}^n (v_{ij} - v_j^+)^2}; D_i^- = \sqrt{\sum_{j=1}^n (v_{ij} - v_j^-)^2}; \quad (9)$$

Step 6: Determination of the Performance Index (PI_i). The relative closeness to the ideal solution is determined by:

$$PI_i = \frac{D_i^-}{D_i^+ + D_i^-} \quad (10)$$

where $0 \leq PI_i \leq 1$. An alternative with a PI_i value closer to 1 indicates a superior multi-objective performance.

Step 7: Final ranking the experimental runs are ranked in descending order of their PI_i values to identify the optimal CMT-WAAM parameter set.

D. GRA Method

Grey Relational Analysis (GRA), derived from grey system theory, is a powerful technique for solving multi-objective optimization problems with limited or uncertain information. It evaluates the degree of similarity between experimental sequences and an ideal reference sequence. For the 20-layer Inconel-718 deposition, the GRA procedure is implemented through the following four steps:

Step 1: Normalization of experimental results (z_{ij}). To ensure comparability, the data are transformed into a dimensionless range using the following criteria:

For "Larger-the-better" criteria (EW, TH):

$$z_{ij} = \frac{x_{ij} - \min(x_{ij})}{\max(x_{ij}) - \min(x_{ij})} \quad (11)$$

For "Smaller-the-better" criteria (Sa):

$$z_{ij} = \frac{\max(x_{ij}) - x_{ij}}{\max(x_{ij}) - \min(x_{ij})} \quad (12)$$

where x_{ij} is the original experimental value.

Step 2: Calculation of the deviation sequence ($\Delta_{0i}(j)$). The deviation sequence represents the absolute difference between the reference sequence ($z_{0j} = 1$) and the normalized data:

$$\Delta_{0i}(j) = |z_{0j} - z_{ij}| = |1 - z_{ij}| \quad (13)$$

Step 3: Calculation of the Grey Relational Coefficient (GRC). The GRC (GRC_{ij}) quantifies how close z_{ij} is to the ideal value:

$$GRC_{ij} = \frac{\Delta_{\min} + \zeta \Delta_{\max}}{\Delta_{0i}(j) + \zeta \Delta_{\max}} \quad (14)$$

where Δ_{\min} and Δ_{\max} are the minimum and maximum values of the deviation sequence, respectively. The distinguishing coefficient ζ is typically set to 0.5.

Step 4: Computation of the Grey Relational Grade (GRG). The GRG (GRG_i) is the weighted average of the GRCs and serves as the single multi-objective performance index:

$$GRG_i = \sum_{k=1}^n w_j \cdot GRC_{ij} \quad (15)$$

5. Weighting Schemes Implemented

For comparative analysis, two distinct weighting schemes were applied to both TOPSIS and GRA methods:

Scheme 1: Entropy-based weights (objective). Weights are derived from the experimental data dispersion using the EWM procedure described in Section 2. These weights reflect the relative importance of each response based on its information content.

Scheme 2: Equal weights (subjective). All three responses are assigned identical weights: $w_{EW} = w_{TH} = w_{Sa} = 1/3$. This

scheme treats all criteria with equal importance regardless of data variability.

The complete optimization procedure was implemented in MATLAB R2023a. The resulting rankings from the four optimization scenarios (TOPSIS with entropy weights, TOPSIS with equal weights, GRA with entropy weights, and GRA with equal weights) were compared to identify the most robust and reliable parameter combination for CMT-WAAM of Inconel 718 thin walls.

IV. RESULTS AND DISCUSSION

This section analyzes the experimental results of 20-layer Inconel 718 thin walls fabricated by CMT-WAAM. The effects of wire feed speed (wfs) and travel speed (v) on geometric responses and surface quality are examined, followed by multi-objective optimization using TOPSIS and GRA.

1. Statistical analysis

Analysis of variance (ANOVA) was performed using Minitab software at a 95% confidence level, where a P-value below 0.05 indicates statistical significance. The ANOVA results, summarized in Table IV, reveal that both wire feed speed (wfs) and travel speed (v) exert significant effects on all three response variables.

TABLE IV. ANOVA for EW, TH, Sa

Response	EW (mm)		TH (mm)		Sa (μm)	
	Contribution	P-Value	Contribution	P-Value	Contribution	P-Value
Regression	94.93%	0.000	99.16%	0.000	88.58%	0.001
wfs (m/min)	65.45%	0.000	39.43%	0.000	18.92%	0.02
v (cm/min)	29.48%	0.001	59.72%	0.000	69.67%	0.001
Error	5.07%		0.84%		11.42%	
Total	100.00%		100.00%		100.00%	

For effective width (EW), both parameters are statistically significant, with wfs being the dominant factor contributing 65.45% of the total variance, compared to 29.48% for v . The regression model for EW is expressed in Equation (16), with an R^2 value of 94.93%, indicating good model reliability.

$$EW = 4.583 + 0.998 * wfs - 0.0670 * v \quad (16)$$

Regarding total height (TH), travel speed is the most influential factor, accounting for 59.72% of the variance, while wfs contributes 39.43%. The regression model for TH is given in Equation (17), achieving a high R^2 of 99.16%, which demonstrates excellent predictive capability.

$$TH = 38.004 + 1.792 * wfs - 0.2205 * v \quad (17)$$

For surface roughness (Sa), travel speed again exhibits the strongest influence, contributing 69.67% of the variance, whereas wfs contributes 18.92%. The regression model for Sa is presented in Equation (18), with an R^2 of 88.58%, adequately capturing the main trends.

$$Sa = 162.64 + 3.46 * wfs - 0.664 * v \quad (18)$$

Figure 3 illustrates the main effects and interaction effects of wfs and v on the three responses. The main effects plots confirm the ANOVA results: wfs exhibits a steep positive slope for EW , while v shows a moderate negative slope; for TH , v displays a strong negative slope; and for Sa , v shows a pronounced negative slope. The interaction plots reveal that the

effect of wfs on EW becomes more pronounced at lower v, while the combination of high wfs and low v results in the highest Sa due to excessive heat accumulation.

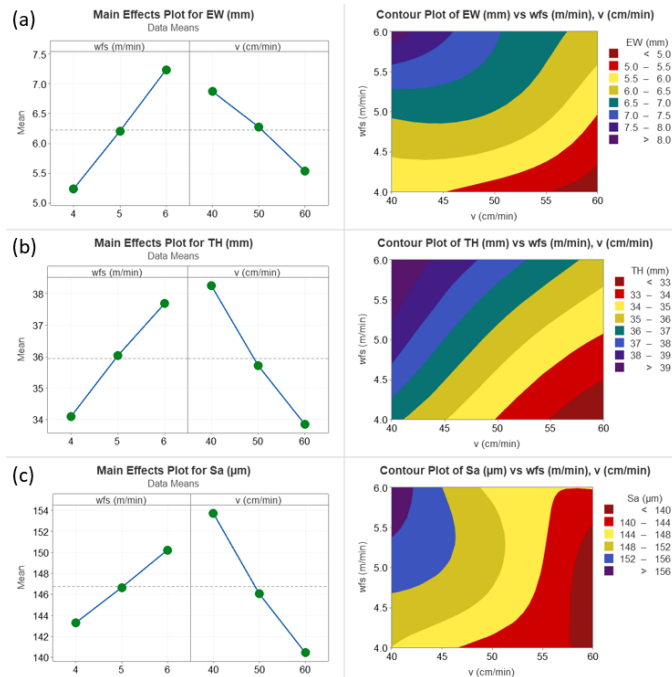


Figure 3. Main effects and interaction effects of wfs and v on (a) effective width (EW), (b) total height (TH), and (c) surface roughness (Sa)

2. Multi-objective optimization results

To resolve the trade-off between deposition efficiency (EW, TH) and surface quality (Sa), a multi-criteria decision-making framework was employed. The Entropy Weight Method (EWM) was first utilized to objectively determine the relative importance of each response based on the inherent dispersion of the experimental data. The calculated entropy values (e_j), diversification degrees (d_j), and final weights (w_j) are summarized in Table V.

TABLE V. Computing the entropy weights for the responses

Criterion	Entropy (e_j)	Diversification (d_j)	Weight (w_j)
Effective Width (EW)	0.9941	0.0059	0.797
Total Height (TH)	0.9990	0.0010	0.135
Surface Roughness (Sa)	0.9995	0.0005	0.068
Total			1.000

The results indicate that effective width (EW) received the highest weight (0.797), followed by total height (TH) (0.135) and surface roughness (Sa) (0.068). This confirms that geometric consistency, particularly lateral expansion—is the most sensitive criterion for 20-layer CMT-WAAM deposition of Inconel 718.

The multi-objective optimization results obtained using the TOPSIS method are shown in Table VI.

The multi-objective optimization results obtained using the GRA method are shown in Table VII.

The results demonstrate a perfect correlation between TOPSIS and GRA. Run 7 (wfs = 6 m/min, v = 40 cm/min) is decisively identified as the optimal processing condition, achieving the highest performance index ($PI_i=0.9780$) and grey

relational grade ($GRG_i=0.9547$). Conversely, Run 3 (wfs = 4 m/min, v = 60 cm/min) is consistently ranked as the least favorable condition for multilayer Inconel 718 buildup.

TABLE VI. TOPSIS optimization results

Run	Parameters		TOPSIS			
	wfs (m/min)	v (cm/min)	D_i^+	D_i^-	PI_i	Rank
1	4	40	0.1105	0.0414	0.2725	6
2	4	50	0.1287	0.0232	0.1528	8
3	4	60	0.1508	0.0030	0.0195	9
4	5	40	0.0718	0.0792	0.5244	3
5	5	50	0.0766	0.0744	0.4925	4
6	5	60	0.1176	0.0336	0.2223	7
7	6	40	0.0034	0.1508	0.9780	1
8	6	50	0.0524	0.0984	0.6526	2
9	6	60	0.0829	0.0680	0.4506	5

TABLE VII. GRA optimization results

Run	Parameters		GRA				
	wfs (m/min)	v (cm/min)	GRC_{EW}	GRC_{TH}	GRC_{Sa}	GRG	Rank
1	4	40	0.4419	0.5603	0.4851	0.4607	6
2	4	50	0.4034	0.4727	0.6134	0.4271	8
3	4	60	0.3333	0.3333	0.7065	0.3588	9
4	5	40	0.5123	0.7473	0.4010	0.5365	3
5	5	50	0.4981	0.5238	0.4674	0.5002	4
6	5	60	0.4190	0.4691	1.0000	0.4654	5
7	6	40	1.0000	1.0000	0.3333	0.9547	1
8	6	50	0.5901	0.6261	0.5049	0.5893	2
9	6	60	0.4767	0.5193	0.5592	0.4880	7

To investigate the influence of weighting selection, an additional optimization was performed using equal weights (1/3 for each response). Table VIII summarizes the TOPSIS and GRA results under this balanced framework.

TABLE VIII. TOPSIS and GRA Results with Equal Weights

Run	wfs (m/min)	v (cm/min)	TOPSIS (PI_i)	Rank	GRA (GRG_i)	Rank
1	4	40	0.3277	6	0.4786	9
2	4	50	0.231	8	0.4848	8
3	4	60	0.18	9	0.4977	6
4	5	40	0.5433	3	0.5534	4
5	5	50	0.487	4	0.4884	7
6	5	60	0.3017	7	0.5943	2
7	6	40	0.8014	1	0.7778	1
8	6	50	0.6532	2	0.5831	3
9	6	60	0.4642	5	0.5215	5

Under equal weights, both TOPSIS and GRA consistently identify Run 7 (wfs = 6 m/min, v = 40 cm/min) as the optimal condition. This result is identical to the entropy-weighted results, confirming that Run 7 is a robust and superior solution regardless of the weighting scheme. Run 7 achieves the maximum effective width (EW = 8.30 mm) and total height (TH = 39.91 mm), albeit with the poorest surface roughness (Sa = 159.42 μ m) due to excessive heat accumulation at low travel speed. Despite this drawback in surface quality, its overwhelming advantage in geometric productivity outweighs the surface finish penalty, even when all three criteria are weighted equally. In contrast, Run 8 (wfs = 6 m/min, v = 50 cm/min) ranks second, offering a better surface finish (Sa = 147.02 μ m) at the cost of slightly lower dimensions (EW = 7.06

mm, TH = 37.58 mm). The only noticeable difference between the two weighting schemes appears in the GRA suboptimal ranking: with equal weights, GRA elevates Run 6 (wfs = 5 m/min, v = 60 cm/min) to second place due to its superior surface roughness ($S_a = 137.37 \mu\text{m}$), indicating that GRA is more sensitive to the surface quality criterion compared to TOPSIS.

V. CONCLUSION

This study systematically investigated and optimized the process parameters for 20-layer deposition of Inconel 718 thin walls using the CMT-WAAM process. Two multi-criteria decision-making methods—TOPSIS and GRA—were applied with two different weighting schemes (entropy weights and equal weights). The following conclusions are drawn:

- Influence of process parameters: Wire feed speed (wfs) is the dominant factor affecting effective width (EW), contributing 65.45% of the total variance. Travel speed (v) primarily governs total height (TH) and surface roughness (S_a), contributing 59.72% and 69.67%, respectively.
- Objective weighting: The Entropy Weight Method assigned weights of 0.797 (EW), 0.135 (TH), and 0.068 (S_a), indicating that geometric consistency—particularly lateral expansion—is the most critical criterion for multi-layer Inconel 718 deposition.
- Optimal solution with entropy weights: Both TOPSIS and GRA unanimously identified Run 7 (wfs = 6 m/min, v = 40 cm/min) as the optimal condition, achieving the highest performance index (0.9780) and grey relational grade (0.9547).
- Robustness under equal weights: When equal weights (1/3 each) were applied, Run 7 remained the optimal solution in both TOPSIS and GRA, confirming its robustness and superiority regardless of the weighting scheme. The only minor discrepancy was observed in GRA suboptimal ranking, where Run 6 (wfs = 5 m/min, v = 60 cm/min) ranked second due to its superior surface roughness ($S_a = 137.37 \mu\text{m}$), indicating that GRA is more sensitive to the surface quality criterion.
- Methodological robustness: The high consistency between TOPSIS and GRA under both weighting schemes confirms the reliability of the proposed optimization framework for CMT-WAAM of Inconel 718 thin-walled components.

ACKNOWLEDGMENT

The authors would like to express their sincere gratitude to Dr. Le Van Thao (Advanced Technology Center, Le Quy Don Technical University) for his valuable guidance and technical contributions throughout this research. The authors also gratefully acknowledge the Faculty of Mechanical Engineering, the Advanced Technology Center, and the Center for Measurement and Testing for providing experimental facilities and equipment, particularly the CMT-WAAM system and the ATOS Q 3D optical scanner, which enabled the successful completion of this work.

REFERENCES

- [1] Price, S., Judd, K., Gleason, M., Tsaknopoulos, K., Cote, D. L., and Neamtu, R. "Advancing Wire Arc Directed Energy Deposition: Analyzing Impact of Materials and Parameters on Bead Shape," *Metals*, vol. 14, no. 3, pp. 282, 2024.
- [2] Zhang, H., Li, Y., Guo, J., Liu, Y., Gao, Z., Chang, T., Fang, X., Nie, L., and Huang, K. "Bead overlapping under oscillatory mode during wire-arc directed energy deposition of superalloy: Investigation on microstructure and mechanical properties," *Materials Science and Engineering: A*, vol. 946, pp. 149130, 2025.
- [3] Farias, F. W. C., Duarte, V. R., Da Cruz Payão Filho, J., Figueiredo, A. R., Schell, N., Maawad, E., Alves Da Fonseca, F. M., Cormier, J., Ramirez, A. J., Santos, T. G., and Oliveira, J. P. "Ni-based superalloy 718 fabricated by arc-based directed energy deposition: an experimentally-based strengthening mechanisms analysis," *Materials Science and Engineering: A*, vol. 939, pp. 148417, 2025.
- [4] Shi, J., Qian, N., Sun, S., Kaynak, Y., Das, R., Fu, Y., and Su, H. "Effect of process parameters on microstructure and properties of Inconel-718 superalloy fabricated by wire-arc direct energy deposition technique," *Journal of Materials Research and Technology*, vol. 37, pp. 173–185, 2025.
- [5] Mattered, G., Caggiano, A., and Nele, L. "Energy Efficiency Optimisation in Wire arc Additive Manufacturing of Invar 36 Alloy via Intelligent Data-Driven Techniques," *International Journal of Precision Engineering and Manufacturing-Green Technology*, vol. 12, no. 3, pp. 905–917, 2025.
- [6] Siddiqui, N. A., Muzamil, M., Jamil, T., and Hussain, G. "Heat sources in wire arc additive manufacturing and their impact on macro-microstructural characteristics and mechanical properties – An overview," *Smart Materials in Manufacturing*, vol. 3, pp. 100059, 2025.
- [7] Doan Tat, K., Le, V. T., and Duong Van, N. "Prediction models and multi-objective optimization of the single deposited tracks in laser direct metal deposition of 316L stainless steel," *Manufacturing Review*, vol. 11, pp. 14, 2024.
- [8] De Lima, J. S., Da Silva Neto, J. F., Maciel, T. M., López, E. A. T., De Santana, R. A. C., and De Abreu Santos, T. F. "Effect of wire arc additive manufacturing parameters on geometric, hardness, and microstructure of 316LSi stainless steel preforms," *The International Journal of Advanced Manufacturing Technology*, vol. 131, no. 12, pp. 5981–5996, 2024.
- [9] Advanced Technology Center, Le Quy Don Technical University, Dinh, D. M., Lam, H. S., Mechanical Electrical Engineering 151, VN, Le, V. T., ATC, Le Quy Don Technical University, 236 Hoang Quoc Viet, Bac Tu Liem, Hanoi, Pham, Q. H., and ATC, Le Quy Don Technical University "Evaluation of the forming quality of Inconel 625 thin-walled parts manufactured via cold metal transfer additive manufacturing," *Science & Technology Development Journal*, 2024.
- [10] Zhang, Z., Yan, J., Lu, X., Zhang, T., and Wang, H. "Optimization of porosity and surface roughness of CMT-P wire arc additive manufacturing of AA2024 using response surface methodology and NSGA-II," *Journal of Materials Research and Technology*, vol. 24, pp. 6923–6941, 2023.
- [11] Kindermann, R. M., Roy, M. J., Morana, R., Francis, J. A., and Prangnell, P. B. "Wire-arc directed energy deposition of Inconel 718: Effects of heat input and build interruptions on mechanical performance," *Additive Manufacturing*, vol. 76, pp. 103765, 2023.
- [12] Huan, P.-C., Wang, X.-N., Zhang, Q.-Y., Di, H.-S., Chen, X.-M., Chen, Y., and Wei, X. "Study on droplet transition behavior, bead geometric characteristics and formability of wire + arc additively manufactured Inconel 718 alloy by using CMT MIX+ Synchronpulse process," *Journal of Materials Research and Technology*, vol. 17, pp. 1831–1841, 2022 .
- [13] Moradi, M., Hasani, A., Pourmand, Z., and Lawrence, J. "Direct laser metal deposition additive manufacturing of Inconel 718 superalloy: Statistical modelling and optimization by design of experiments," *Optics & Laser Technology*, vol. 144, pp. 107380, 2021.
- [14] Jiang, F., Sun, L., Huang, R., Jiang, H., Bai, G., Qi, X., Liu, C., Su, Y., Guo, C., and Wang, J. "Effects of Heat Input on Morphology of Thin-Wall Components Fabricated by Wire and Arc Additive Manufacturing," *Advanced Engineering Materials*, vol. 23, no. 4, pp. 2001443, 2021 .
- [15] Alonso, U., Veiga, F., Suárez, A., and Gil Del Val, A. "Characterization of Inconel 718® superalloy fabricated by wire Arc Additive Manufacturing: effect on mechanical properties and machinability,"



Journal of Materials Research and Technology, vol. 14, pp. 2665–2676, 2021.

- [16] Alinezhad, A. and Khalili, J. “New Methods and Applications in Multiple Attribute Decision Making (MADM),” *in* vol. 277, 2019.